Journal of Applied Fluid Mechanics, Vol. 15, No. 3, pp. 747-756, 2022.
Available online at www.jafmonline.net, ISSN 1735-3572, EISSN 1735-3645.
https://doi.org/10.47176/jafm.15.03.33138

Analysis on the Performances of Misaligned Journal Bearings using Full-Scale Test Rig and Conjugate Heat Transfer Method

Q. Li†, Y. J. Du, Y. J. Wang, S. Zhang, Q. L. Liu, B. Li and W. W. Xu

College of New Energy, China University of Petroleum (East China), Qingdao, 266580, China

†*Corresponding Author Email: liqiangsydx@163.com*

(Received June 26, 2021; accepted December 27, 2021)

ABSTRACT

Misalignment effects increase the risk of scratch or seizure failure for the journal bearings-rotor system. To investigate the performances of misaligned journal bearings, a full-scale journal bearings-rotor system test rig is designed and journal orbits are tested under different speeds. Then, a THD lubrication model is established to simulate lubrication performances under different misalignment conditions. The results show that for a misaligned journal bearings-rotor system, the center of the orbits of the bearing closing to coupling is fixed around the coupling. The orbits center of the bearing far away coupling is floating gradually with an increasing speed. The vibration amplitude of bearing closing to coupling is larger than that of bearing far away from the coupling. When the minimum oil film thickness is decreasing, the maximum film temperature is increasing except for the bearing closing to coupling. For different misalignment directions, maximum film temperature is determined by the position of the high pressure zone and high temperature zone.

Keywords: Journal bearings; Misalignment; Full-scale test rig; Computational fluid dynamics; Conjugate heat transfer.

NOMENCLATURE

B	bearing length	R_e	vapor generation rate
c	conductivity	S_h	volumetric heat sources
C_e, C_c	empirical constants	T	temperature
d_b	bearing diameter	T_{in}	inlet temperature
d_j	journal diameter	T_{max}	maximum film temperature
$\boldsymbol{F}$	body force	$\boldsymbol{v_m}$	mass-averaged velocity
f_g	noncondensable gases mass fraction	W	loading capacity
f_v	vapor mass fraction	α	angle of attack
h_{min}	minimum oil film thickness	γ	dummy variable
k	turbulence kinetioc energy	θ	angular coordinate
L_1	length between bearing 1# and coupling	μ_m	viscosity of mixture
L_2	length between bearing 2# and coupling	μ_l	Viscosity of liquid
N	speed	μ_v	viscosity of vapor
n	number of phases	ρ_m	density of mixture
p_v	liquid saturation vapor pressure	ρ_l	density of liquid
p_{in}	inlet pressure	ρ_v	density of vapor
R_c	vapor condensation rate	σ	surface tension coefficient of the liquid

1. INTRODUCTION

Hydrodynamic journal bearings are widely used in rotating systems, predominantly in centrifugal compressors and pumps (Alves *et al*. 2019). The lubrication performance of journal bearings has significant effects on the efficiency and reliability of the machinery (Li *et al*. 2020). Misalignment of the shaft and bearing houses can be caused by shaft deformation under heavy load, non-central loading, manufacturing errors, or improper installation (Zhang *et al*. 2016). As the second most common malfunction after unbalance, misalignment has a considerable influence on the lubrication and

dynamic characteristics of the journal bearings-rotor system (Sun *et al*. 2014).

For the experimental investigation, there are two strategies in designing an experiment rig for understanding the performances of a journal bearings-rotor system with misalignment. The first strategy is that the shaft was supported by the tested journal bearing and assisted bearings (Prabhu *et al*. 1997; Beamish *et al*. 2020). The assisted bearings were used to achieve the initial alignment. Then, a special component was designed to apply load, which led to a specified misalignment condition. This rig type is commonly used for lubrication testing and cannot reflect the dynamic misalignment condition. To investigate the dynamic behavior of a misaligned journal bearings-rotor system, the second strategy arranged the journal bearings-rotor testing system as same as real rotating machinery. Hu *et al*. (2000) developed a rig for lateral misalignment investigation of multi journal bearings-rotor system. Then, Sun *et al*. (2019) presented the shaft shape errors on the instability of two journal bearings - rotor system. However, the scale of this rig type is small, and extending these tests to full-scale applications remains a challenge (Samyn *et al*. 2006). Moreover, journal orbits have not been presented for a misaligned full-scale journal bearings-rotor system under different rotational speeds.

For the numerical investigation, thermal effects of misalignment journal bearings have drawn attention. Pierre *et al*. (2004) highlighted that misalignment would reduce the pressure and increase the temperature in the bearing mid-plane. Thomsen and Klit (2012) proposed an improved method of journal bearing operation at heavy misalignment using flexible bearings and compliant liners. Sun *et al*. (2010) considered a misaligned plain journal bearing with a rough surface and highlighted that the surface roughness has an effect on the lubrication performance for a large journal misalignment angle. Zhang *et al*. (2013) developed a comprehensive TEHD (Thermo-elasto-hydrodynamic) model effects and deformations on the behavior of misaligned plain journal bearings. However, the Reynolds equation, which was used for lubrication analysis as the review above, neglected the inertia effect. And this effect has a considerable influence on thermohydrodynamic characteristics of journal bearings (Nassab 2005; Vakilian *et al*. 2013).

Recently, to eliminate this limitation, CFD (Computational fluid dynamics) techniques have been used to solve the exact Navier-Stokes equations (Armentrout *et al*. 2017). For journal bearings, as in many other heat transfer applications, it is necessary to associate heat transfer in the fluid with the heat conduction inside the adjacent solid surfaces. The coupling of these two models of heat transfer is termed CHT (Conjugate Heat Transfer) (Silieti *et al*. 2009). Taking the CHT at the bearing house and rotor into account, a thermohydrodynamic analysis of 3D sector-pad thrust bearings with rectangular dimples was developed by Papadopoulos *et al*. (2014). Then Fouflias *et al*. (2015) completed the performance comparison between textured, pocket, and tapered-land sector-pad thrust bearings. Song and Gu (2015) developed a 3D CFD analysis for hydrodynamic bearings considering both cavitation and conjugate heat transfer effects. Li *et al*. (2017a) and Mo *et al*. (2018) established a new full 3D CFD method, which was applied to tilting pad journal bearings and self-lubricating bearings in gear pumps, respectively. However, to the authors' knowledge, there is no numerical study of misaligned journal bearings based on CHT, except that Zhang *et al*. (2019) presented a TEHD lubricating model of a textured misaligned journal bearing.

In present study, the experimental apparatus of a full-scale journal bearings-rotor system is firstly presented. Further, the misalignment under different speeds is investigated and journal orbits of the misaligned journal bearings-rotor system are given. Finally, THD (thermohydrodynamic) lubrication models based on the CHT method are established to investigate the effect of misalignment on the lubrication performance of journal bearings.

2. DESCRIPTION OF THE EXPERIMENTAL APPARATUS

Figure 1 presents the schematic of full-scale journal bearings-rotor test rig. Bearing close to the coupling is marked as 1# and bearing far from the coupling is marked as 2#. The rotor is supported by two identical full-scale journal bearings and is driven by an 11 kW AC motor with a maximum speed of 8,000 rpm. The AC motor is controlled through a converter and its precision of steady speed is 0.05%. The lubricant is 32# turbine oil and two gear pumps are used to circulate lubricant. The vibration of the rotor is monitored by four eddy current displacement sensors. The sensitivity of the eddy current displacement sensors is 5 V/mm. Then, the generated signals during the test are collected by a signal acquisition card and transmitted to the PC for processing.

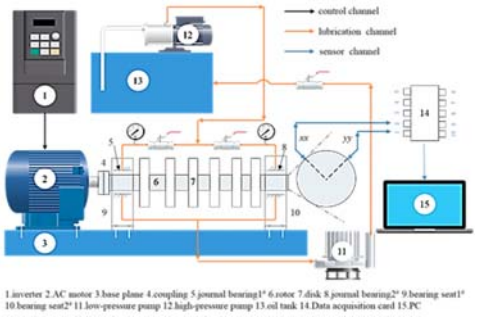

Fig. 1. Schematic of the test rig.

Figure 2 provides a photograph of the mechanical part. In order to accommodate the frequent start and stop conditions, metallic disc coupling is used to combine the shaft of the motor and rotor. The rectangular convexity is designed at the baseplate to achieve the initial alignment of two bearing houses. Each bearing is equipped with two eddies current

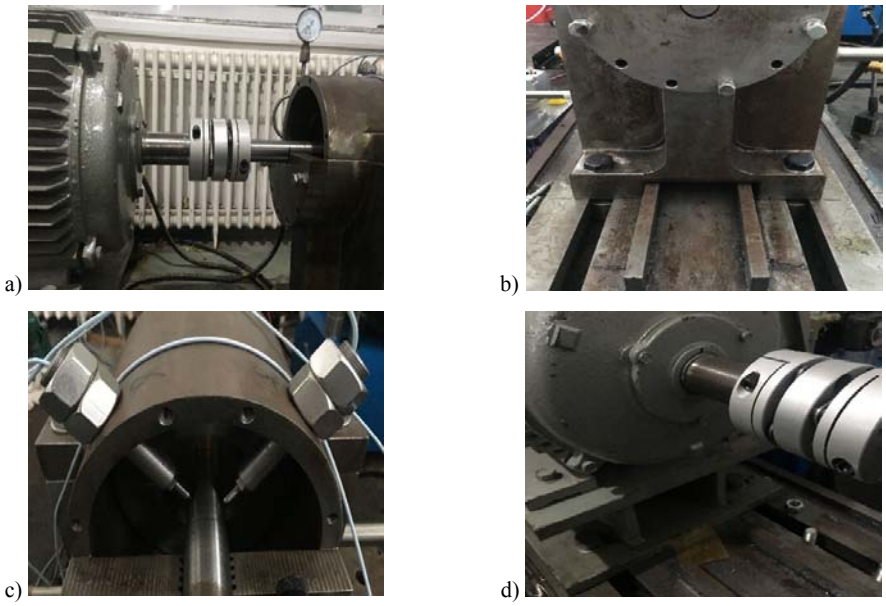

Fig. 2. Photograph of the test rig. a) Metallic disc coupling b) Baseplate c) Sensors installation d) Achievement of an initial misalignment.

Table 1 Parameters used in the numerical analysis.

Symbol	Parameters	Value
μ_v	viscosity of vapor	2.0×10^{-5} Pa·s
ρ_l	density of liquid	850 kg/m^3
ρ_v	density of vapor	1.2 kg/m^3
pv	liquid saturation vapor pressure	29185 Pa
d_b	bearing diameter	50.1 mm
d_j	journal diameter	50.0 mm
B	bearing length	25.0 mm
N	rotational speed	3000 r/min
p_{in}	inlet pressure	0.1 MPa
T_{in}	inlet temperature	313K

displacement sensors at right angles for journal orbits testing.

The entire assembling process is similar to the assembling process of centrifugal compressors and pumps. In order to eliminate the effect of the initial imbalance on the vibration test of the rotor, a dynamic balancing test of the rotor system is carried out at a speed of 3000 r/min using an influence coefficient method with trial weights. A thin sheet of copper is placed on the bottom of the motor for an initial misalignment, as shown in Fig. 2(d). After that, the orbits at two journal bearings of this misaligned journal bearings-rotor system are tested at speeds of 2000 r/min, 2500 r/min, 3000 r/min, 3500 r/min, 4000 r/min, and 4500 r/min respectively. Using 2000 r/min as an example, firstly, the motor is started. Secondly, when the required speed 2000r/min is achieved and the motor runs steadily, the data is acquired. Intermediate data from the test result are analyzed to ensure data reliability. Then the speed is increased gradually, and the above procedure is repeated until the completion of the test.

3. NUMERICAL METHOD

3.1 Physical model and boundary conditions

Figure 3 shows the physical model in present study. The lubricant enters the bearing from the "inlet" at the central plane and flows out from the "outlet" at axial ends. The parameters of the journal bearing are listed in Table 1.

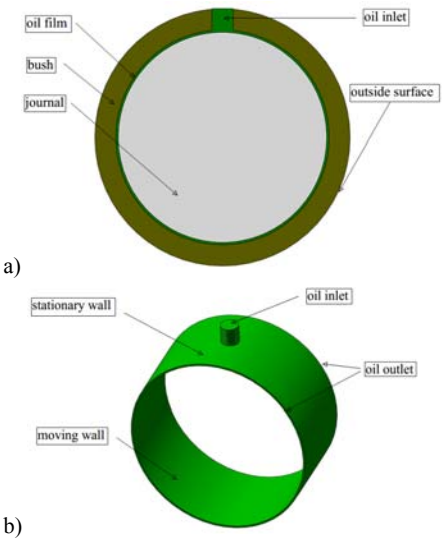

Fig. 3. Physical model. a) Journal bearing b) Oil film.

The meshes for the fluid and solid domain can be seen in Fig. 4, including both the fluid domain and the solid domain, as shown in Fig. 4 (a) and (b), respectively. The fluid domain is used to simulate the flow field, and the solid domain mainly takes the heat conduction and heat transfer into account.

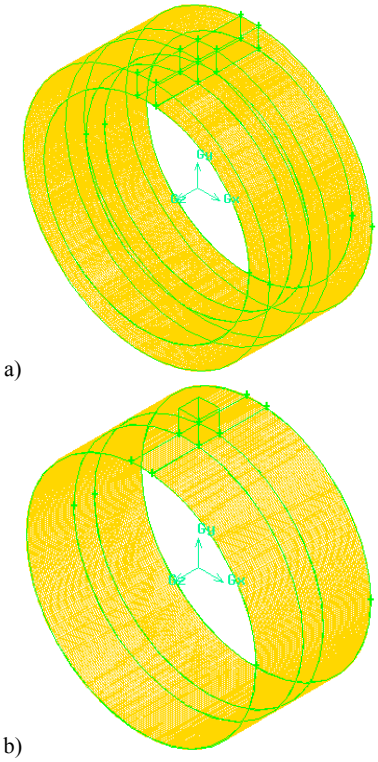

Fig. 4. Meshes for the fluid and solid domains. a) Solid domain b) Fluid domain.

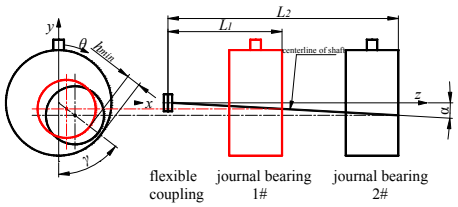

Fig. 5. Schematic of misaligned journal bearings-rotor system.

To model the CHT effect, a coupled heat transfer of the bearing house and oil film domain is used. A zero heat flux thermal boundary is imposed on the moving wall. This results in the same grid divisions for the fluid and structural parts in the axial and circumferential directions. A square cross section instead of a circular one is used at the inlet tube for simplification and the whole domain can be meshed with a hexahedral type element. And the dynamic meshing method previously proposed by Li *et al.* (2017b) is used to update the mesh to consider the squeezed and deformed of the oil film.

Grid independence verification has already finished in Li *et al.* (2018). After the grid convergence test, the mesh density cases used in the axial and circumferential directions are 190 and 1220 divisions, and in the radial direction, the oil film is divided into 5 layers.

Figure 5 shows the schematic of misaligned journal bearings-rotor system. Misalignment condition is represented by two parameters h_{min} and γ. γ is the misalignment direction and h_{min} is the minimum film thickness at a given γ. Taking the coupling position as reference, the pressure and temperature distribution are investigated under different h_{min} and γ.

3.2 Governing equations of CHT

Firstly, the "Mixture" model is used to describe the multiphase flow of lubricant with cavitation. The Singhal *et al.* (2002) model "full cavitation model" is used and the transfer rate is calculated using the following equations:

$$R_e = C_e \frac{\sqrt{k}}{\sigma}\rho_l\rho_v\sqrt{\frac{2(p_v-p)}{3\rho_l}}\left(1-f_v-f_g\right), p \le p_v$$
$$R_c = C_c \frac{\sqrt{k}}{\sigma}\rho_l\rho_l\sqrt{\frac{2(p-p_v)}{3\rho_l}}f_v, p > p_v \quad (1)$$

Where R_e, R_c is the vapor generation rate and vapor condensation rate, C_e, C_c is the empirical constants, k is the turbulence kinetic energy, σ is the surface tension coefficient of the liquid, ρ_l, ρ_v is the liquid and vapor density, p_v is the liquid saturation vapor pressure, f_v is the vapor mass fraction and f_g is the noncondensable gasses mass fraction.

The "Mixture" model solves the continuity equation and momentum equation for the mixture, and the volume fraction equation for the secondary phases.

$$\frac{\partial}{\partial t}\left(\rho_m\right)+\nabla\cdot\left(\rho_m\boldsymbol{v_m}\right)=0 \quad (2)$$

where v_m is the mass-averaged velocity and ρ_m is the mixture density.

$$\frac{\partial}{\partial t}\left(\rho_m\boldsymbol{v_m}\right)+\nabla\left(\rho_m\boldsymbol{v_m}\boldsymbol{v_m}\right)=-\nabla p$$
$$+\nabla\left[\mu_m\left(\nabla\boldsymbol{v_m}+\nabla\boldsymbol{v_m}^T\right)\right]+\rho_m\boldsymbol{g} \quad (3)$$
$$+\boldsymbol{F}+\nabla\left(\sum_{k=1}^{n}\alpha_k\rho_k v_{dr,k}v_{dr,k}\right)$$

where n is the number of phases, F is a body force, and μ_m is the viscosity of the mixture.

$$\frac{\partial}{\partial t}\left(\rho_m f_k\right)+\nabla\left(\rho_m\boldsymbol{v_m}f_k\right)=\nabla\left(\mu_m\nabla f_k\right)+R_e-R_c \quad (4)$$

where f_k is vapor mass fraction of phase k.

Then, when CHT is used to describe the temperature distribution of journal bearings, the energy equation of fluid and solid regions are synchronously solved:

$$\frac{\partial}{\partial t}\sum_{k=1}^{n}(\alpha_k\rho_k E_k)+\nabla\cdot\sum_{k=1}^{n}(\alpha_k \boldsymbol{v_k}(\rho_k E_k+p)) = \nabla\cdot\left(k_{eff}\nabla T\right)+S_h \tag{5}$$

where k_{eff} is the effective conductivity and S_h includes any other volumetric heat sources.

$$\frac{\partial}{\partial t}(\rho h)+\nabla\cdot(\boldsymbol{v}\rho h)=\nabla\cdot(c\cdot\nabla T)+S_h \tag{6}$$

where ρ and c are the density and conductivity of solid region, respectively.

And the continuity of the temperature and normal heat flux are ensured between the fluid and solid regions by:

$$T\big|_F = T\big|_S \tag{7}$$

$$\lambda_F\frac{\partial T}{\partial n}\Big|_F=\lambda_S\frac{\partial T}{\partial n}\Big|_S \tag{8}$$

where T is the temperature of liquid, λ_F and λ_S are thermal conductivity of the fluid and solid respectively.

The material properties of the bearing house are assumed to be temperature independent. The variation of viscosity with temperature is simulated using the Walther viscosity relation (Khonsari and Booser 2008):

$$\log\log(\frac{\mu_l}{\rho_l}+0.7)=10.0032-3.9785\log T \tag{9}$$

where μ_l is the viscosity of liquid.

The solution of above equations is obtained by "SIMPLE" algorithm. For the spatial discretization of pressure, a "PRESTO!" scheme is used. For greater accuracy, a convergence tolerance of 10^{-6} is used for all residual terms.

4. EXPERIMENTAL RESULTS AND DISCUSSION

Figure 6 presents the journal orbits of the full-scale misaligned journal bearings-rotor system under different speeds. Because the copper sheet achieves an initial misalignment at vertical direction, orbits of bearing1# is reasonable higher. The orbits center of bearing 1# is relatively fixed and around the coupling compared with the orbits center of bearing2#. And with the increasing of speed, the orbits center of bearing 2# is floating gradually.

By testing, the first-order critical speed is about 3700 r/min. From 2000 r/min to 3500 r/min, the amplitudes of both journals are increasing. After passing the first-order critical speed, the amplitude is decreasing at 4000 r/min. Then, the amplitude is increasing again at 4500 r/min. Further testing is shut down because of the severe vibration. For this full-scale misaligned journal bearings-rotor test rig, the amplitude of bearing 1# is much larger than that of bearing 2#. The combining effect of the larger amplitude and off-centered orbits will increase the risk of uneven contact and seizure, especially for the bearing close to the coupling.

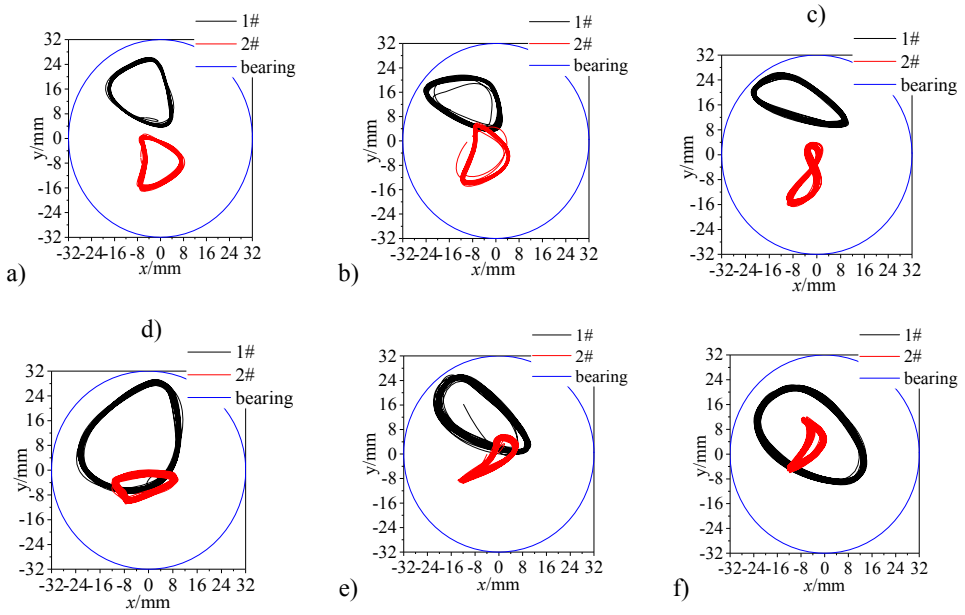

Fig. 6. Journal orbits under different speeds. a) 2000 r/min b) 2500 r/min c) 3000 r/min d) 3500 r/min e) 4000 r/min f) 4500 r/min.

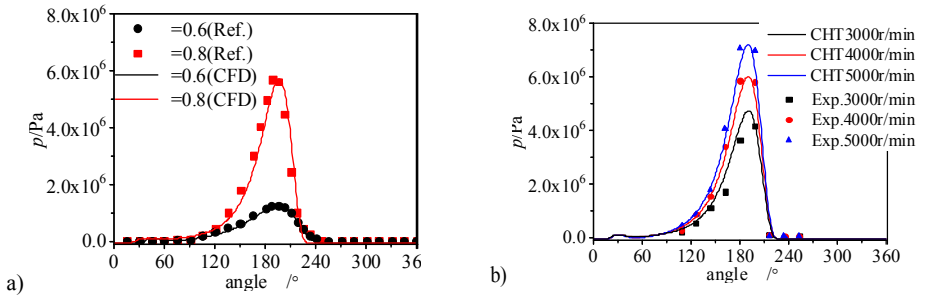

Fig. 7. Comparison of the calculated pressure distribution with reference results. a) Comparison with the numerical results b) Comparison with the experimental results.

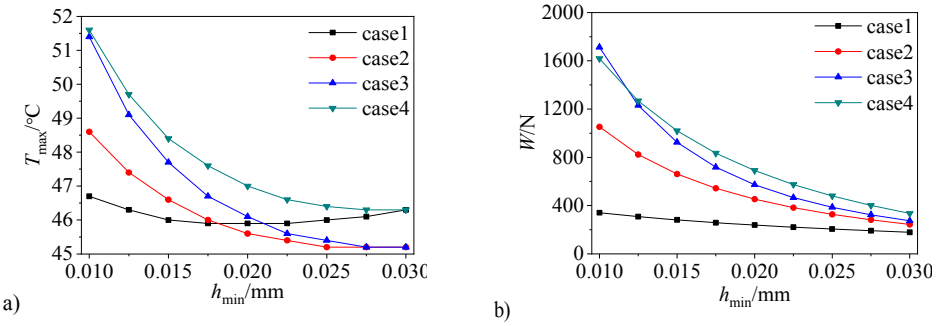

Fig. 8. Effect of minimum oil film thickness h_{min}. a) Maximum film temperature T_{max} b) Loading capacity W.

5. NUMERICAL RESULTS AND DISCUSSION

5.1 Validation study

To our knowledge, the experimental test of pressure and temperature of the oil film is still a challenge because of small clearance, especially for such a full-scale journal bearings-rotor system with complex mechanical structure. Therefore, the validation of present method is based on previous literature. Dhande and Pande (2016) conducted steady-state simulations and experiments on journal bearings and offered detailed test data to validate the calculation results, as shown in Fig. 7, where ε is eccentricity ratio. The simulation results of Dhande and Pande (2016) are based on the isothermal assumption. Therefore, by neglecting the thermal effect, the calculation results of this paper marked by CFD are used to compare with the simulation results. Then, pressure distributions calculated by CHT are compared with experimental results. Reasonable agreements are achieved both in the numerical and experimental results, which illustrates that the CHT method is suitable for lubrication analysis of journal bearings.

5.2 Effect of minimum film thickness

Misalignment amplitude d was introduced to define the severity of misalignment by Pierre *et al*. (2004). If misalignment of journal and bearing exists, minimum oil film thickness h_{min} would be a suitable parameter to reflect the risk of uneven contact. Therefore, the severity of misalignment is represented by h_{min} in present study. And the relationship between d and h_{min} can be expressed:

$$d=\alpha B=\frac{(\frac{d_b-d_j}{2}-h_{\min})}{L}\cdot B$$
$$L=\begin{cases}L_1 & \text{bearing 1\#}\\ L_2 & \text{bearing 2\#}\\ \infty & \text{alignment}\end{cases} \tag{10}$$

where α is misalignment angle, L_1 is the length between bearing 1# and coupling, and L_2 is the length between bearing 2# and coupling.

Four cases listed in Table 2 are analyzed and case 4 is used to analyze the cavitation effect on temperature.

Table 2 Four cases used in the numerical analysis.

case1	case2	case3	case4
misalignment with cavitation of bearing 1#	misalignment with cavitation of bearing 2#	alignment with cavitation	alignment without cavitation

For a given γ=180°, the maximum film temperature T_{max} and loading capacity W against h_{min} are shown in Fig. 8. As shown in Fig. 8(a), T_{max} increases as h_{min} decreases because of the enhancement of viscosity

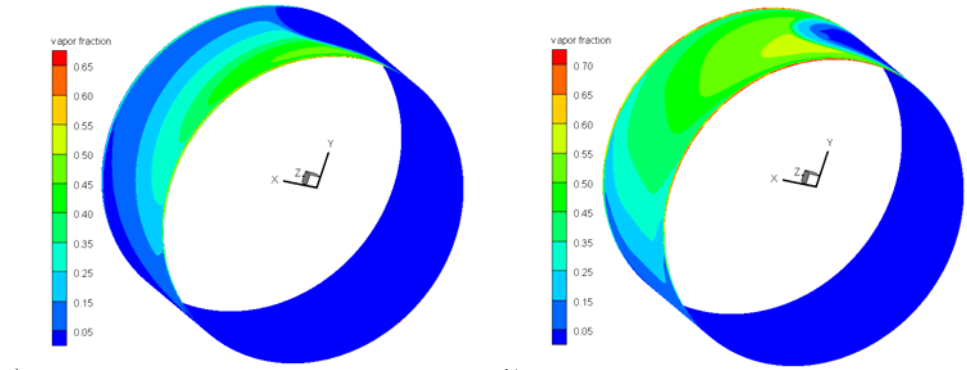

Fig. 9. Cavitation effect of journal bearings under h_{min}=0.03 mm. a) Bearing1# b) Bearing2#.

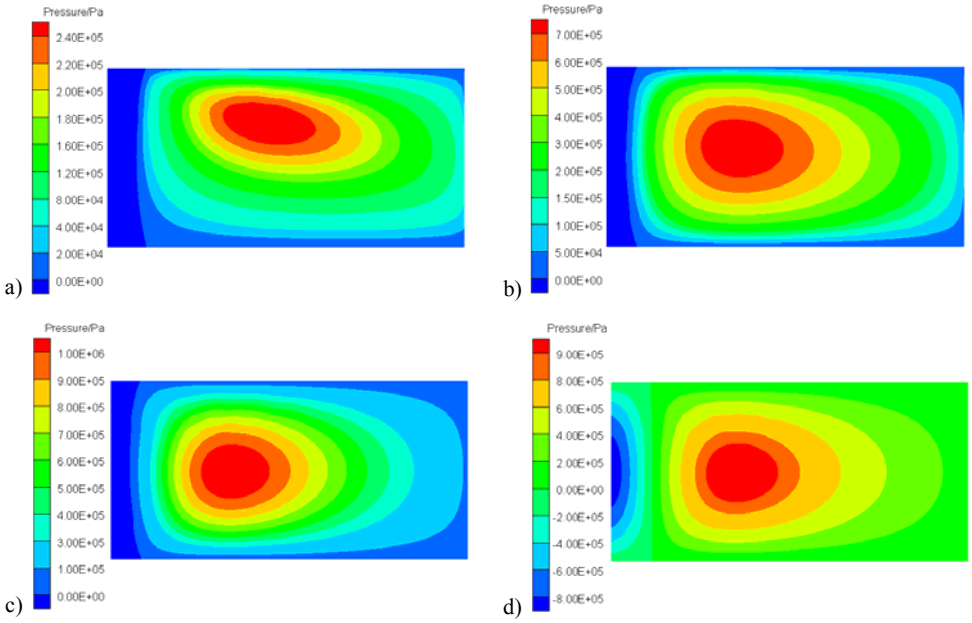

Fig. 10. Pressure distribution against misalignment cases.

a) Case 1 b) Case 2 c) Case 3 d) Case 4

heating for case 2, case 3 and case 4. The findings reported here are congruent with results of Pierre *et al*. (2004) and Thomsen *et al*. (2012). However, for case 1, T_{max} shows a trend of decreasing first and then increasing with the decrease of h_{min}. The trend is due to the cavitation. Cavitation occurs when the oil film could no longer withstand the tension. Then, the lubricant becomes a mixture of liquid oil and oil vapor.

Therefore, the existence of the oil vapor causes a considerable decrease of the viscosity. Further, T_{max} decreases as the decrease of viscosity. The cavitation of the misaligned journal bearings under h_{min} =0.03mm is shown in Fig. 9., it can be found that the cavitation of the journal bearing close to coupling is weakened due to the misalignment. Therefore, the T_{max} has a slightly increasing as h_{min} increases in Bearing1#. As expected, the misalignment leads to a decreasing of loading capacity, as shown in Fig. 8(b). Figure 10 shows pressure distributions for the same h_{min}, it shows that misalignment leads to the movement of the high pressure zone towards the thinner film side, further reduces the loading capacity

5.3 Effect of misalignment direction

Figure 11 presents the maximum film temperature T_{max} and loading capacity W at different misalignment direction γ. For a better explanation, the corresponding contours of temperature and pressure are given in Fig. 12-13. The loading capacity W is minimum around γ=180° because the high pressure zone is destroyed by the inlet position. And maximum film temperature T_{max} is determined

by the position of high pressure zone and high temperature zone.

The high pressure zone exists at the upstream of h_{min} and high temperature zone exists at the downstream of h_{min}. When γ increases from 0° to 150°, the high temperature zone, existing at the upstream of inlet, is getting close to the inlet. Therefore, fresh lubricant is directly heated. Furthermore, the T_{max} is increasing, as described in Fig. 12(a)-(d). Then, around γ=180°, because the high pressure zone is destroyed by the inlet position (Fig. 13(e)), the flow resistance of oil film is sharply dropped, leading to the decreasing of T_{max} (Fig. 12(e)). When γ increases from 210° to 270°, the high temperature zone, existing around the inlet, is gradually faring away from inlet (Fig. 12(f)-(h)) and high pressure zone forms at the downstream of inlet(Fig. 13(f)-(h)). Flow resistance of oil film is gradually increasing. Therefore, T_{max} reaches a peak at γ=270°. When γ increases from 270° to 360°, the high temperature zone is further far away from inlet and T_{max} is dropping.

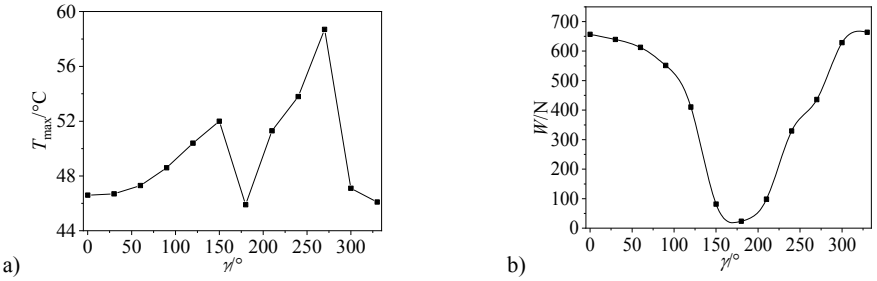

Fig. 11. Influence of misalignment angle γ. a) Maximum film temperature T_{max} b) Loading capacity W.

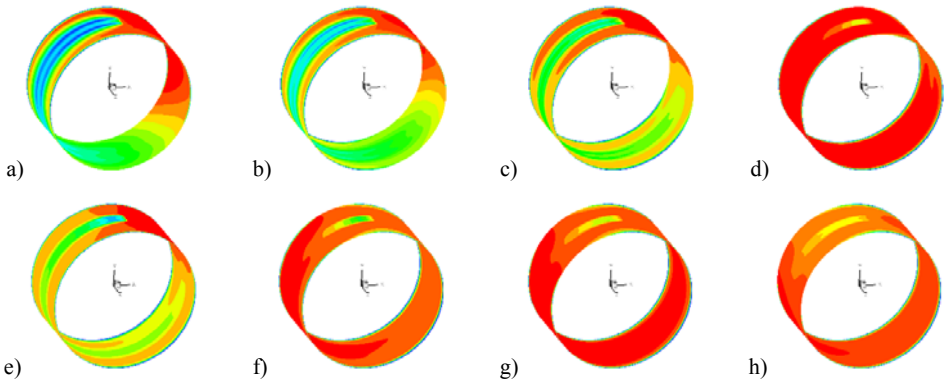

Fig. 12. Contours of temperature against γ. a) γ=60° b) γ=90° c) γ=120° d) γ=150° e) γ=180° f) γ=210° g) γ=240° h) γ=270°.

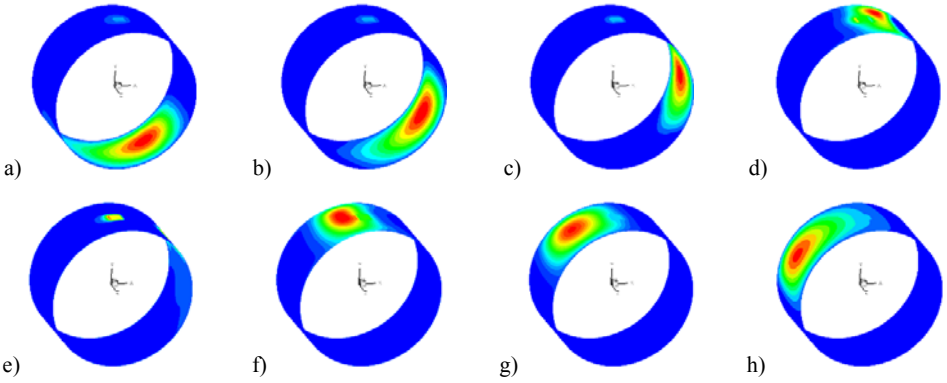

Fig. 13. Contours of pressure against γ. a) γ=60° b) γ=90° c) γ=120° d) γ=150° e) γ=180° f) γ=210° g) γ=240° h) γ=270°.

6. CONCLUSION

In present study, a full-scale journal bearings-rotor system test rig is designed and a THD lubrication model of misaligned journal bearings is established based on CHT method. Then, journal orbits and lubrication performances of rotor-misaligned journal bearings system are investigated. The following conclusions are drawn:

(1) For a misaligned journal bearings-rotor system, the orbits center of the bearing close to coupling is relatively fixed around the coupling. The orbits center of the bearing far away coupling is floating gradually with an increasing speed. The combining effect of the larger amplitude and off-centered orbits will increase the risk of uneven contact and seizure, especially for the bearing close to the coupling.

(2) THD method is a valid method to investigate the temperature distribution of journal bearings and the calculation results show a reasonable agreement with reference.

(3) When minimum oil film thickness is decreasing, maximum film temperature is increasing except the bearing closing to coupling. Because the misalignment in that bearing weakens the cavitation effect, further enhances the viscosity heating.

(4) The misalignment leads to the movement of the high pressure zone towards the thinner film side, further reduces the loading capacity.

(5) For different misalignment directions, maximum film temperature is determined by the position of high pressure zone and high temperature zone. When high temperature zone exists around the inlet and high pressure zone exists at the downstream of the inlet, maximum film temperature will reach a peak.

ACKNOWLEDGEMENTS

This work is supported by the National Natural Science Foundation of China (No.52176050, 51506225), the General Program of Natural Science Foundation of Shandong Province (ZR2020ME174), the Key Research and Development Program of Shandong, China (No. 2018GHY115018), and the Fundamental Research Funds for the Central Universities (No. 18CX02129A).

REFERENCES

Alves, D. S., M. F. Wu and K. L. Cavalca (2019). Application of gain-scheduled vibration control to nonlinear journal-bearing supported rotor. *Journal of Sound and Vibration* 442, 714-737.

Armentrout, R. W., M. He, T. Haykin and A. E. Reed (2017). Analysis of turbulence and convective inertia in a water-lubricated tilting-pad journal bearing using conventional and CFD approaches. *Tribology Transactions* 60(6), 1129-1147.

Beamish, S., X. Li, H. Brunskill, A. Hunter and R. Dwyer-Joyce (2020). Circumferential film thickness measurement in journal bearings via the ultrasonic technique. *Tribology International* 148, 10629.

Dhande, D. Y. and D. W. Pande (2016). Numerical analysis of multiphase flow in hydrodynamic journal bearing using CFD coupled Fluid Structure interaction with cavitation. *International Conference on Automatic Control and Dynamic Optimization Techniques* 964-971.

Fouflias, D. G., A. G. Charitopoulos, C. I. Papadopoulos, L. Kaiktsis and M. Fillon (2015). Performance comparison between textured, pocket, and tapered-land sector-pad thrust bearings using computational fluid dynamics thermohydrodynamic analysis. *Proceedings of the Institution of Mechanical Engineers, Part J: Journal of Engineering Tribology* 229(4),376-397.

Nassab, G. S. A. (2005). Inertia effect on the thermohydrodynamic characteristics of journal bearings. *Proceedings of the Institution of Mechanical Engineers, Part J: Journal of Engineering Tribology* 219(6), 459-467.

Hu, W., H. Miah, N. S. Feng and E. J. Hahn (2000). A rig for testing lateral misalignment effects in a flexible rotor supported on three or more hydrodynamic journal bearings. *Tribology International* 33(3), 197-204.

Khonsari, M. M. and E. R. Booser (2008). Applied Tribology: Bearing Design and Lubrication: Second Edition. *John Wiley and Sons* 1-566.

Li, H., H. Liu, S. Qi and Y. Liu (2020), A high-speed rolling bearing test rig supported by sliding bearing. *Industrial Lubrication and Tribology* 72(7), 955-959.

Li, M. X., S. Zheng, G. Ying and Q. Li (2017a). Development and validation of the 3D temperature field simulation for the tilting pad journal bearings. *Computational Thermal Sciences* 9(2), 151-163.

Li, Q., S. Zhang, L. Ma, W. W. Xu and S. Y. Zheng (2017b). Stiffness and damping coefficients for journal bearing using the 3D transient flow calculation. *Journal of Mechanical Science and Technology* 31(5), 2083-2091.

Li, Q., S. Zhang, Y. J. Wang, W. W. Xu and Z. B. Wang (2018). Investigations of the three-dimensional temperature field of journal bearing considering conjugate heat transfer and cavitation. *Industrial Lubrication and Tribology* 71(1), 109-118.

Mo, J. T., C. Gu, X. Pan, S. Zhen and G. Ying (2018). A Thermohydrodynamic Analysis of the Self-Lubricating Bearings Applied in Gear Pumps Using Computational Fluid Dynamics Method. *Journal of Tribology* 140(1), 011102.

Papadopoulos, C. I., L. Kaiktsis and M. Fillon (2014). Computational fluid dynamics thermohydrodynamic analysis of three-dimensional sector-pad thrust bearings with rectangular dimples. *Journal of Tribology* 136(1), 011702.

Pierre, I., J. Bouyer and M. Fillon, (2004). Thermohydrodynamic behavior of misaligned plain journal bearings: theoretical and experimental approaches. *Tribology Transactions* 147(4) 594-604.

Prabhu, B. S. (1997). An experimental investigation on the misalignment effects in journal bearings.

Tribology Transactions 40(2), 235-242.

Samyn, P., P. De Baets, G. Schoukens and A. P. Van Peteghem (2006). Large-scale tests on friction and wear of engineering polymers for material selection in highly loaded sliding systems. *Materials and Design* 27(7) 535-555.

Silieti, M., A. J. Kassab and E. Divo (2009). Film cooling effectiveness: Comparison of adiabatic and conjugate heat transfer CFD models. *International Journal of Thermal Sciences* 148，2237-2248.

Singhal, A. K., M. M. Athavale, H. Y. Li and Y. Jiang (2002) Mathematical basis and validation of the full cavitation model. *Journal of Fluids Engineering-Transactions of the ASME* 124(3), 617-624.

Song, Y. and C. Gu (2015). Development and validation of a three-dimensional computational fluid dynamics analysis for journal bearings considering cavitation and conjugate heat transfer. *Journal of Engineering for Gas Turbines and Power* 137(12), 122502.

Sun, F. X., X. Zhang, X. Wang, Z. Su and D. Wang (2019). Effects of shaft shape errors on the dynamic characteristics of a rotor-bearing system. *Journal of Tribology-Transactions of the ASME* 141(10), 101701.

Sun, J., M. Deng, Y. Fu and C. Gui (2010). Thermohydrodynamic lubrication analysis of misaligned plain journal bearing with rough surface. *Journal of Tribology* 132(1), 1-8.

Sun, J., X. Zhu, L. Zhang, X. Wang, C. Wang, H. Wang and X. Zhao (2014). Effect of surface roughness, viscosity-pressure relationship and elastic deformation on lubrication performance of misaligned journal bearings. *Industrial Lubrication and Tribology* 66(3), 337-345.

Thomsen, K. and P. Klit (2012). Improvement of journal bearing operation at heavy misalignment using bearing flexibility and compliant liners. *Proceedings of the Institution of Mechanical Engineers, Part J: Journal of Engineering Tribology* 226(8), 651-660.

Vakilian, M., S. A. G. Nassab and Z. Kheirandish (2013). Study of inertia effect on thermohydrodynamic characteristics of Rayleigh step bearings by CFD method. *Mechanics and Industry* 14(4), 275-285.

Zhang, X. L., Z. Yin, D. Jing, G. Gao, Y. Wang and X. Wang (2016). Load carrying capacity of misaligned hydrodynamic water-lubricated plain journal bearings with rigid bush materials. *Tribology International* 99, 1-13.

Zhang, Y., G. Chen and L. Wang (2019). Thermoelastohydrodynamic analysis of misaligned bearings with texture on journal surface under high-speed and heavy-load conditions. *Chinese Journal of Aeronautics* 32(5), 1331-1342.

Zhang, Z. S., X. Dai and Y. Xie (2013). Thermoelastohydrodynamic behavior of misaligned plain journal bearings. *Proceedings of the Institution of Mechanical Engineers, Part C: Journal of Mechanical Engineering Science* 227(11), 2582-2599.